Available online at www.sciencedirect.com

SCIENCE DIRECT®

Journal of Molecular Catalysis A: Chemical 200 (2003) 191–203

JOURNAL OF MOLECULAR CATALYSIS A: CHEMICAL

www.elsevier.com/locate/molcata

Catalytic air oxidation of ambient temperature hydrocarbons

Melvin Keith Carter*

Carter Technologies, P.O. Box 1852, Los Gatos, CA 95031, USA

Received 2 January 2003; received in revised form 21 January 2003; accepted 28 January 2003

Abstract

Catalytic air oxidation of the aliphatic hydrocarbons *n*-decane, hexanes, gasoline and diesel fuel was conducted at ambient temperature with novel iron catalysts. The concentration of *n*-decane in water was reduced from 1.42 g in 100 ml to 0.07 g in 100 ml in 5 h at room temperature forming carbon monoxide and water by means of intermediate aldehydes. Results of FT–IR and GC–MS analyses demonstrated formation of aldehydes and unsaturated alcohols. Carbon monoxide was detected on catalyst residues and in the vapor phase. The indicated catalytic reaction mechanisms are discussed.

Keywords: Air oxidation; *n*-Decane; Hexanes; Gasoline; Diesel fuel; Aldehydes; Unsaturated alcohols; Catalyst

1. Introduction

Aliphatic hydrocarbons are oxidized by high temperature combustion, chemical oxidizing agents used with transition metal catalysts [1–5] and by shaped pore silicate structures [6–12] also requiring elevated temperatures. Elevated temperature oxidations of aliphatic hydrocarbons apparently pass through carboxylic acids forming carbon dioxide and water. This report describes ambient temperature catalytic air oxidation of aliphatic hydrocarbons forming carbon monoxide and water by means of intermediate aldehydes.

Hydrocarbons are subject to radical attack in forming oxidized products. A peroxo radical intermediate [13,14] has been proposed for chemical oxidation of liquid alkanes to alcohols, aldehydes and ketones by means of alkyl hydroperoxides. Peroxide oxidation of alcohols with Fe(II) has been investigated in detail [15–17] and has been described [18] as involving a hydroxy radical $^{\bullet}OH$ or its kinetic equivalent the ferryl radical (FeO^{1+} or $FeOH^{2+}$, where un-neutralized charges are indicated) [15]. Catalytic oxidations are fast ($<10^{-12}$ s) such that radical species are not detected. Transition metal catalysts, such as di-nuclear iron oxo-bridge complexes, have been suggested as possible model catalyst precursors [19–22] in place of Fe(II) or Fe(III). Methane mono-oxygenase enzyme, which reportedly contains two adjacent iron complexes each with an Fe–Fe bond distance of 0.34 nm [23,24] as probable catalytic sites, air oxidizes methane at ambient temperature. The present article reports catalytic air oxidation of liquid hydrocarbons at ambient temperature and pressure using novel iron catalysts.

2. Catalyst considerations

Oxidative catalysts were designed applying the principles developed previously [25]. An ambient

* Corresponding author. Tel.: +1-408-356-6693; fax: +1-408-356-9633.
E-mail address: mkcarter@ix.netcom.com (M.K. Carter).

1381-1169/03/$ – see front matter
doi:10.1016/S1381-1169(03)00098-0

Table 1
Relative bonding energies for first row transition metal complexes

Transition metal complex[a]	ΔE (eV)	ΔE (kcal/mol)
$Ti_2(O_2)_4^{4+}$	+0.0003	<+0.1
$V_2(O_2)_4^{4+}$	+0.6128	+14.1
$Cr_2(O_2)_4^{4+}$	+0.5327	+12.3
$Mn_2(O_2)_4^{4+}$	−0.1193	−2.7
$Fe_2(O_2)_4^{4+}$	+0.0482	+1.1
$FeCl_4^{2-}(O_2)_4FeCl_4^{2-}$[b]	−6.476	−149
$Co_2(O_2)_4^{4+}$	−0.2455	−5.7
$Ni_2(O_2)_4^{4+}$	−0.2312	−5.3
$Cu_2(O_2)_4^{4+}$	−0.9114	−21.0

[a] The optimized distances were d(M–M) = 0.2482 nm, d(O–O) = 0.125 nm.
[b] Bond distance for Fe–Cl is 0.265 nm and Cl–Fe–Cl bond angle is 102°.

temperature air oxidation catalyst precursor, $Fe(CN)_2L\cdot Fe(CN)_2L$ for L being $K_3Cu(CN)_4$ and related ligands, was selected for oxidation of aliphatic hydrocarbons because this linear Fe–Fe backbone met the bonding symmetry requirement for catalysts [25]. An acceptable oxidation mechanism, involving a catalyst with dual iron strings of two iron atoms per string, was established and metal–O_2 bonds formed in the presence of water (Step 1), refer to Table 1. The Fe–Fe backbone was linear (Step 2) and an approximate bonding energy to the associated oxygen reactant was computed (Step 3). The lowest valence state for which the energy values were two-fold degenerate was 2+ (Step 4). Pairs of cyanide and chloride ions were chosen as chemically compatible with the Fe in formation of a catalyst precursor (Step 5). The rule of 18 electrons [26] was not met so compatible ligands of the form $K_3Cu(CN)_4$ were added to complete the coordination shell. In this case the catalytic iron ion contributed six 3d-electrons, each cyanide ion contributed two 2p-electrons, two of the complexed cyanide ligands contributed two electrons each and the adjacent transition metal contributed four 3d-electrons for a total of 18 electrons (Step 6). Replacement of the ligands, L, by similar groups also produced active catalysts. An approximate associated bonding energy of −16 kcal/mol (−67 kJ/mol) was computed for the catalyst–oxygen association with the ligands present, which was in the 5–60 kcal/mol range as required.

3. Experimental

3.1. Catalyst preparation

Preparation of iron oxidation catalysts followed the six-step design process described in Section 2. All steps in the catalyst preparation were conducted using nitrogen sparging and nitrogen blanketing in sealed plastic containers to minimize air oxidation of the transition metal compounds [27]. The following solutions were prepared using a minimum volume of DI water but not <15 mL total. An aqueous solution of 1.0420 g (0.016 mol) of KCN was added to a solution of 1.5904 g (0.008 mol) of $FeCl_2\cdot 4H_2O$ with agitation from bubbling nitrogen forming a red–orange colored suspension. To 0.7165 g (0.008 mol) of powdered CuCN was added 1.0419 g (0.016 mol) of KCN dissolved in minimal deionized water. This mixture was heated to boiling producing a clear solution of $K_2Cu(CN)_3$, was cooled and added to the first solution producing a tan colored suspension. The solid was acidified with 0.436 g of 75% phosphoric acid, allowed to settle, was drained, washed with five 30 ml portions of nitrogen purged water, drained again and vacuum dried producing a tan colored solid identified as Catalyst A.

Catalyst B, a bright yellow solid, was prepared by a similar process replacing the $K_2Cu(CN)_3$ ligand with $K_3Cu(CN)_4$ formed from 0.7166 g (0.008 mol) of copper(I) cyanide and 1.5630 g (0.024 mol) of KCN dissolved in minimal deionized water with boiling. Exposure of Catalyst B to air produced a dark blue colored solid identified as oxidized Catalyst B.

Catalysts A and B were both allowed to settle for a day, the clear liquid layer removed under nitrogen and replaced with de-ionized water. This exchange process was repeated several times more until relatively clean solid catalyst suspensions were obtained. The solids were isolated by filtration and dried under nitrogen. These catalysts were insoluble in hot concentrated sulfuric acid and aqua regia, at elevated pressures and temperatures in a microwave reactor. They were digested in a 1:8 $NaNO_3$:NaOH molten flux followed by dissolution in hot 1:1 hydrochloric acid in preparation for elemental analyses and metals analysis by ICP. Results of these analyses are presented in Tables 2–3. FT–IR spectra were recorded for KBr pellets of Catalyst A and oxidized Catalyst B.

Table 2
Model of mixed catalyst compounds representing $Fe(CN)_2L{\cdot}Fe(CN)_2L$

Weight	C	N	Cu	Fe	K
Experimental (anal.)	0.1601	0.1857	0.1594	0.1637	0.3232
0.45 $Fe(CN)_2{\cdot}Fe(CN)_2{\cdot}2K_3Cu(CN)_4$ + 0.25 $Fe(CN)_2{\cdot}Fe(Cl)_2{\cdot}K_3Cu(CN)_4$ + 0.30 $K_3Fe(OH)_3(CN)_3$ equivalent to 0.70 $2Fe(CN)_2{\cdot}1.7K_3Cu(CN)_4{\cdot}2KCl$					
Calculated	0.1602	0.1868	0.1521	0.1623	0.2908

An FT–IR spectrum of the light colored solid Catalyst A displayed three absorption bands located at 2095, 2050 and 585 cm^{-1}. The doublet absorption at 2095 and 2050 cm^{-1} was interpreted as CuCN and FeCN absorption's, respectively [28]. The band located at 585 cm^{-1} was indicative of ionic transition metal cyanides [29], such as $Fe(CN)_6{}^{4-}$. An FT–IR spectrum of the deep blue oxidized Catalyst B also displayed three absorption bands at 2075, 595 and 460 cm^{-1}. The bands at 2075 and 595 cm^{-1} were identified as the ionic cyanide absorption [28] and the band located at 460 cm^{-1}, which was present in oxidized samples but was essentially absent for the prepared yellow Catalyst B, indicated Fe(OH) absorption [29].

3.2. Catalytic air oxidation of n-decane

n-Decane was catalytically oxidized in ambient air as described. To a 250 mL beaker was added 100 ml of DI water and 1.42 g of +99% pure *n*-decane oil (10 mmol, 14,000 ppm). Catalyst B was prepared as described and 1 mmol of the catalyst suspension was dispersed into the water with rapid stirring at 16+1 °C and atmospheric air pressure to start the reaction as the catalyst color became deep blue. Twelve 1 mL samples were collected for analysis during the first 5 h run with the last one being collected just prior to a subsequent 1.42 g addition of *n*-decane. Each 1 mL sample was immediately extracted by vigorous agitation for 30 s with 2 ml of reagent grade dichloromethane. The concentrations of residual *n*-decane and oxidized hydrocarbon products were measured by a GC procedure for each extract. Refer to results listed in Table 4. This provided the residual concentration of hydrocarbon, showing its rate of consumption, and remaining concentration of oxidized products, as shown in Fig. 1. The suspensions for high concentrations of *n*-decane defined quantitative collection for concentrations above ~5000 mg/kg although lower concentrations appeared to be quantitative. Therefore, two additional reactions were conducted, one for 15 min and the other for 30 min, after which the entire mixture of each was immediately extracted to isolate and collect

Table 4
Concentration of *n*-decane and remaining products

Reaction time (h)	Decane remaining (gm/100 mL)	Products in water (mg/100 mL)
0.00	1.42	0.00
0.25	1.27	2.82
0.50	0.500	13.3
0.75	0.460	6.29
1.02	0.435	6.85
1.51	0.379	–
2.00	0.314	5.56
2.51	0.250	–
3.02	0.223	6.90
3.50	0.129	–
4.00	0.153	5.08
4.50	0.129	–
5.00	0.073	1.61
45	0.07	1.6

Table 3
Model of mixed catalyst compounds representing $Fe(CN)_2L'{\cdot}Fe(CN)_2OH$

Weight	C	N	Cu	Fe	K
Experimental (anal.)	0.1704	0.1974	0.1495	0.2352	0.1848
0.75 $Fe(CN)_2OH{\cdot}Fe(CN)_2{\cdot}K_2Cu(CN)_3$ + 0.13 $Fe(CN)_2OH{\cdot}Fe(Cl)_2{\cdot}K_2Cu(CN)_3$ + 0.12 $Fe(CN)_2OH{\cdot}Fe(Cl)_2{\cdot}2K_2Cu(CN)_3$					
Calculated	0.1704	0.1987	0.1472	0.2309	0.1811

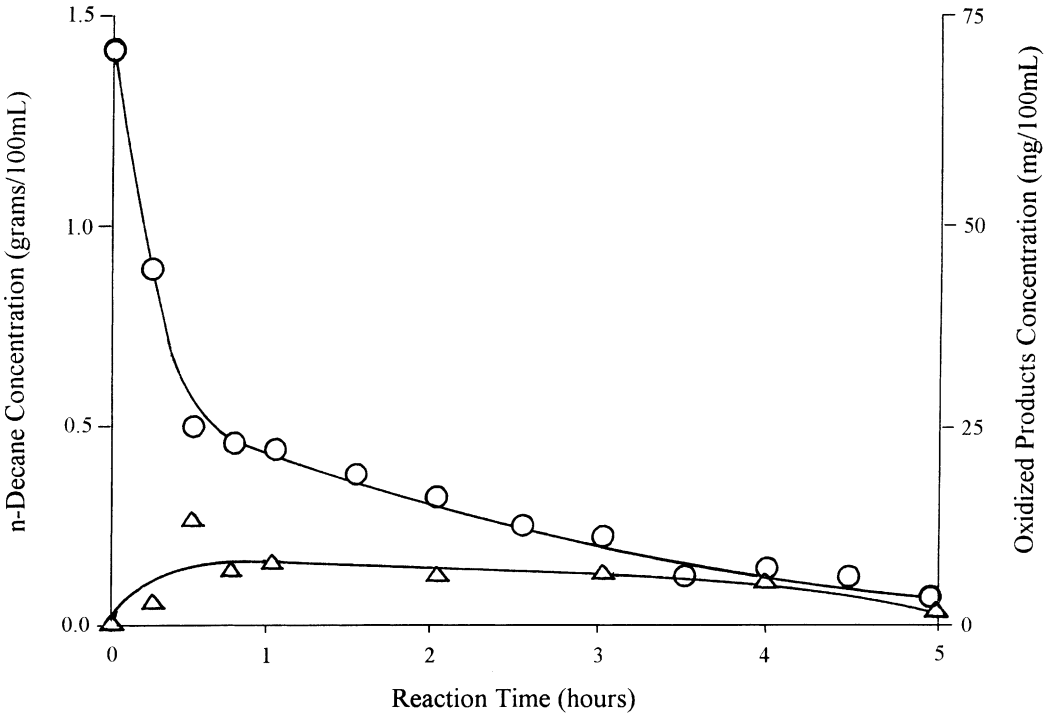

Fig. 1. Catalytic air oxidation of *n*-decane as a function of time, the curve through the open circles represents measured concentrations of *n*-decane. The curve through the triangles represents the sum of measured concentrations of oxidized products.

all organic products for analysis. Catalytic air oxidation reactions were continued with sequential additions of 1.42 g of *n*-decane following each additional 5 h reaction period for a total of nine sequential additions. The entire aqueous solution was repeatedly extracted after the final 5 h catalytic oxidation period yet approximately 70 mg of product was recovered for measurement by GC–MS (fit with a 30 m Carbowax megabore capillary column), refer to data in Table 5.

Table 5
Major GC–MS peaks of oxidized *n*-decane after 5 h (initial reaction)

Peak no.	Mass (Da)	Formula
1	392	$C_{26}H_{48}O_2$
2	280	$C_{18}H_{32}O_2$
3	282	$C_{19}H_{38}O$
4	282	$C_{19}H_{38}O$
5	280	$C_{18}H_{32}O_2$

The evaporation rate of 1.424 g of *n*-decane was measured at 16 + 1 °C under these same rapid stirring conditions with no catalyst present. At the end of 5 h the weight of residual extracted *n*-decane was 1.24 g showing that 0.178 g of *n*-decane had been lost due to evaporation and/or mechanical means.

n-Decane was also oxidized in a sealed 25 L Tedlar gas sampling bag enclosure to trap the volatile organic products formed in the first 90 min of catalyzed air oxidation of 1.42 g of *n*-decane using 2 mmol of catalyst. Operating conditions established a reactant temperature of 30 + 2 °C. The entire 25 L volume of air and product gases were slowly passed through an absorption tube containing reagent grade dichloromethane to isolate volatile organic compounds. Less than 3 mg of oxidized products and substantial *n*-decane were recovered from the tube extract for measurement and approximately 70 mg of product was recovered from the liquid. The GC–MS analysis demonstrated the vaporized products to be in the C_4–C_{10} range and products from the water phase to be in the C_7–C_{11}

Table 6
GC–MS peaks of *n*-decane oxidized in enclosed atmosphere for 90 min

Peak no.	Liquid sample		Vapor sample	
	Mass (Da)	Formula	Mass (Da)	Formula
1	126	$C_7H_{10}O_2$	56	C_3H_4O
2	142	$C_9H_{18}O$	86	$C_4H_6O_2$
3	156	$C_{10}H_{20}O$	100	$C_6H_{12}O$
4	154	$C_{10}H_{18}O$	142	$C_8H_{14}O_2$
5	156	$C_{10}H_{20}O$	120	C_9H_{12}
6	156	$C_{10}H_{20}O$	134	$C_{10}H_{14}$
7	154	$C_{10}H_{18}O$	156	$C_{10}H_{20}O$
8	170	$C_{11}H_{22}O$	174	$C_9H_{18}O_3$
9	148	$C_{11}H_{16}$		
10	148	$C_{11}H_{16}$		
11	186	$C_{11}H_{22}O_2$		
12	174	$C_9H_{18}O_3$		

range, refer to data in Table 6. The aqueous portion was carefully reduced to dryness at 80 °C and a KBr pellet formed for recording an FT–IR spectrum. Results indicated –OH stretch at 3449 cm^{-1}, –OH motion at 1379 and 1058 cm^{-1}, $–CN^-$ motion at 2088, 2047 and 586 cm^{-1} for the catalyst bonding, linear CO chelation motion at 2088 and 2047 cm^{-1}, and metal formate M–COOH bond motions at 1655 and 1622 cm^{-1}. Trace level hydrocarbon absorption indicated <0.1% of the catalyst weight was associated with hydrocarbon or oxidized hydrocarbon products. The evaporation rate of 1.428 g of *n*-decane was measured under these same 30 + 2 °C conditions with no catalyst present. At the end of 1.5 h, the weight of residual extracted *n*-decane was 0.040 g showing that 1.388 g of *n*-decane had evaporated.

Another sealed 25 L Tedlar bag catalytic oxidation was run as described previously to trap gases formed during the first 90 min of catalytic air oxidation of 1.42 g of *n*-decane. The trapped air and product gases were sampled in duplicate using Drager tubes to quantitate for carbon monoxide, acrolein and formaldehyde. No formaldehyde was detected (<1 ppm), but 50 ppm of carbon monoxide was detected and 27 ppm of acrolein was measured and listed in Table 6. All gases were expelled from the Tedlar bag and the interior walls were extracted with 75 ml of reagent grade ethanol. The extract was allowed to evaporate at ambient temperature (10–16 °C) for 5 days. The residue was weighed repeatedly during the final stages of evaporation until it changed more slowly with time. This knee in the evaporation curve, 0.043 g, was identified as an end point for determination of residue absorbed on the enclosure walls although some volatiles were probably lost.

A third 90 min experiment was conducted in a sealed 25 L Tedlar bag as discussed previously. The entire 25 L of air and product gases were slowly bubbled through 50 ml of 2 M sodium hydroxide solution to absorb carbon dioxide and other gaseous products formed during the catalytic oxidation reaction. Titration of the alkaline solution with 1 M sulfuric acid to a pH 5.2 end point accounted for <5 mg of carbon dioxide.

3.3. Catalytic air oxidation of hexanes at ambient pressure

Catalytic oxidation of hexanes, using Catalyst B, was conducted at atmospheric pressure under the same conditions as described for *n*-decane except that a round bottom flask was fit with a cold trap condenser cooled with a dry ice–acetone mixture. Catalytic hexanes consumption was equivalent to evaporative loss. The GC–MS analysis demonstrated the recoverable products to be similar to those of Section 3.2. Lower molecular weight compounds, eluting close to the solvent peak, eluded detection. Refer to Table 7.

Table 7
Major GC–MS peaks of oxidized hexanes (at 1 atm)

Peak no.	Mass (Da)	Formula
1	98	$C_6H_{10}O$
2	214	$C_{12}H_{22}O_3$
3	256	$C_{16}H_{32}O_2$
4	282	$C_{17}H_{30}O_3$
5	276	$C_{17}H_{34}O_3$
6	296	$C_{19}H_{36}O_2$
7	310	$C_{21}H_{42}O$
8	324	$C_{21}H_{40}O_2$
9	358	$C_{23}H_{34}O_3$
10	366	$C_{24}H_{46}O_2$
11	372	$C_{27}H_{46}$
12	394	$C_{26}H_{50}O_2$
13	414	$C_{26}H_{54}O_3$
14	400	$C_{25}H_{52}O_3$
15	310	$C_{21}H_{42}O$
16	282	$C_{18}H_{34}O_2$

3.3.1. Catalytic air oxidation of hexanes at 7.1 atmospheres pressure

Volatile hexanes were oxidized using a pressurized stainless steel reactor to retain all products. To 5.54 L of water containing 200 ppm of hexanes (dispersed in the water by rapidly injecting a 2:1 methanol solution of hexanes) was added 3.9 g (∼2 mmol) of an aqueous dispersion of Catalyst A. This aqueous mixture was quickly transferred to a stainless steel chamber by pumping thereby compressing the trapped air to 0.69 MPa (105 psig, 7.1 atm) gauge pressure. The water was rapidly circulated for 30 min, while being agitated using a 1 kW ultrasonic driver, during which time the temperature incidentally increased from 18 to 53 °C. The water and products were allowed to cool for 24 h in the reactor. The reactor was opened and the entire volume was extracted with a total of 100 mL of reagent grade dichloromethane, in three equal batches, combined and reduced to a 20 mL volume for analysis. The extract was analyzed for products by FT–IR (Fig. 2) and GC–MS (Fig. 3) procedures. Refer to the GC–MS analysis information in Table 8.

An FT–IR spectrum recorded for the extract residue of hexanes oxidized at 7 atm pressure, refer to Fig. 2, exhibited aliphatic hydrocarbon absorption bands located at 2955 cm^{-1} for a CH_3– stretch, 2923 and 2852 cm^{-1} for –CH_2– stretch, 1463 cm^{-1} for –CH_2– deformation, 1377 cm^{-1} for a CH_3–C deformation, 1249 and 805 cm^{-1} for $(CH_3)_3$–C motion and a band located at 720 cm^{-1} for –$(CH_2)_4$– motion. Catalyst–aldehyde association bands were observed [28] at 1301, 1183 and 1042 cm^{-1}. Aldehyde C–H stretch bands were observed at 2729 and 2670 cm^{-1}, an aldehyde C–H deformation band at 830 cm^{-1} and an aliphatic aldehyde C=O stretch band located at 1735 cm^{-1}. There was a C=O stretch band located at 1717 cm^{-1}, a deformation band at 1608 cm^{-1},

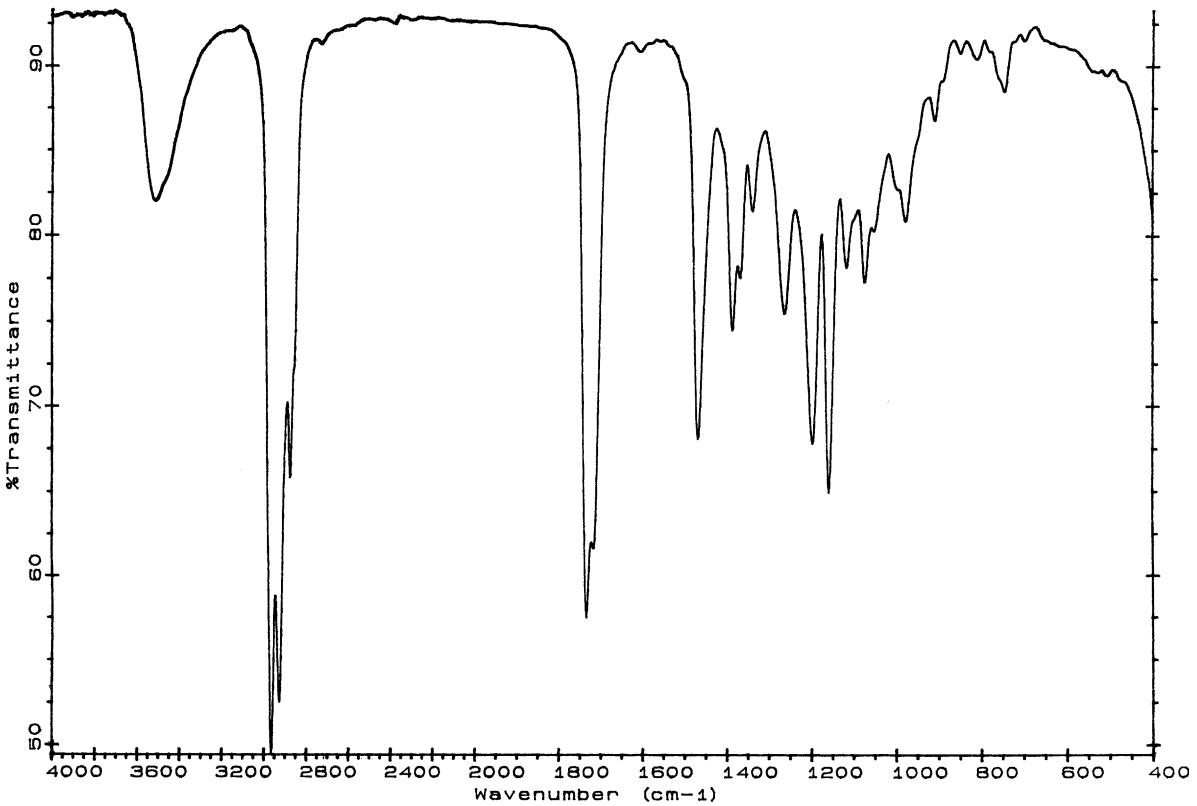

Fig. 2. FT–IR of hexane product residue.

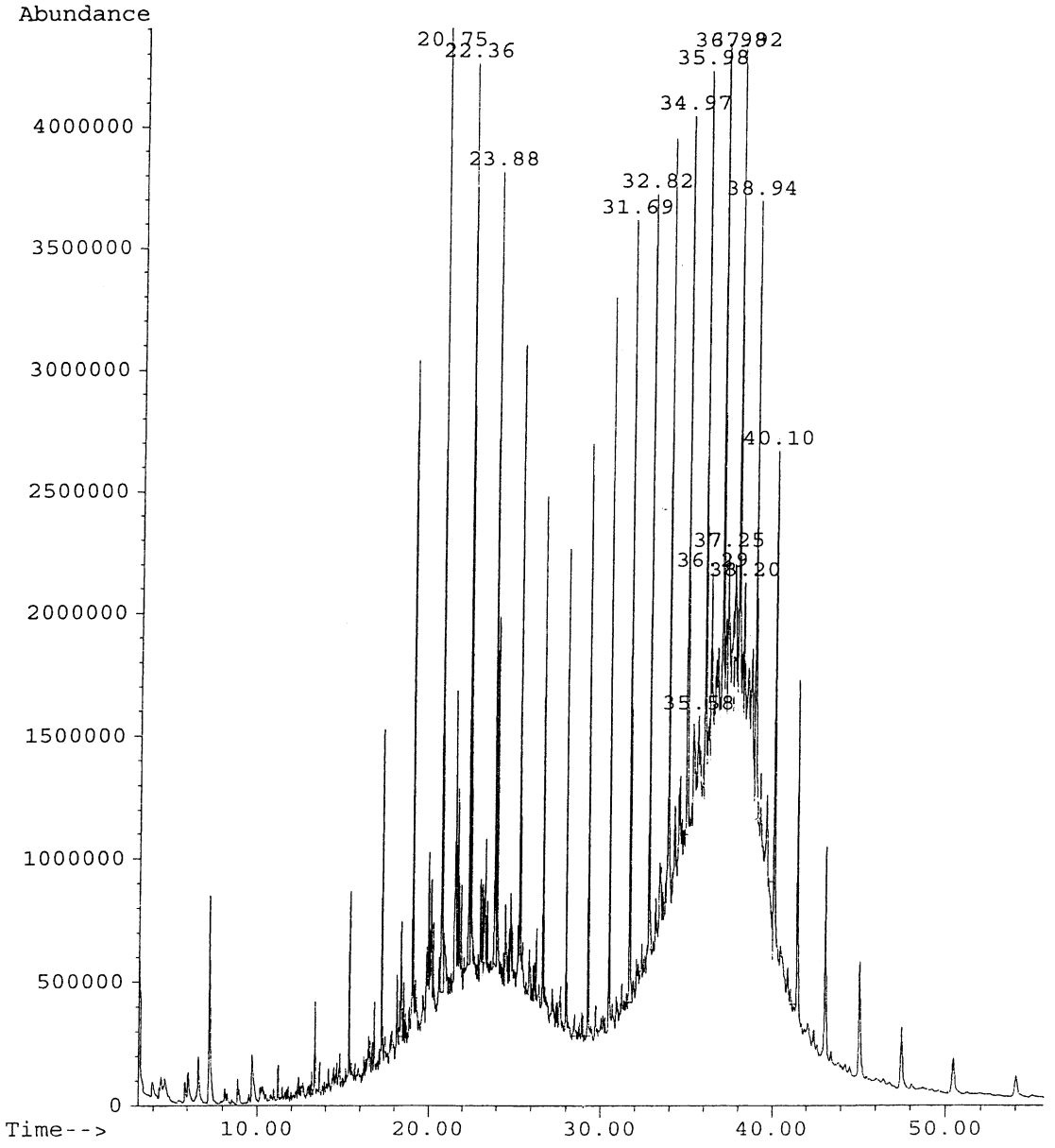

Fig. 3. GC–MS of hexane products.

a –C=O deformation band located at 1366 cm^{-1} and an HO– out-of-plane deformation band located at 890 cm^{-1}. The weaker band at 1717 cm^{-1} may be indicative of an unsaturated aliphatic aldehyde or ketone while the band at 1608 cm^{-1} is indicative of a metal formate. There were also three weak, well formed absorption bands located at 1559, 1541 and 1509 cm^{-1} which were attributed to –C=O–Fe aldehyde–catalyst chelation bands [29] having a bond energy of 14.6 kJ/mol (3.5 kcal/mol). Absorption near 1515 cm^{-1} is attributed to substituted carbon–carbon bond unsaturation.

Table 8
Major GC–MS peaks of oxidized hexanes (at 7.1 atm)

Peak no.	Elution time (min)	Mass (Da)	Formula
1	13.7	114	$C_6H_{10}O_2$
2	15.3	134	$C_6H_{14}O_3$
3	17.1	170	$C_9H_{18}O_2$
4	18.3	184	$C_{10}H_{20}O_2$
5	19.0	198	$C_{11}H_{22}O_2$
6	20.0	192	$C_{14}H_{24}$
7	20.7	212	$C_{13}H_{24}O_2$
8	21.5	222	$C_{14}H_{22}O_2$
9	22.3	226	$C_{15}H_{30}O$
10	23.3	234	$C_{15}H_{22}O_2$
11	24.0	236	$C_{15}H_{24}O_2$
12	24.7	240	$C_{16}H_{32}O$
13	25.2	236	$C_{15}H_{24}O_2$
14	26.0	238	$C_{16}H_{30}O$
15	26.7	254	$C_{17}H_{34}O$
16	27.9	248	$C_{17}H_{28}O$
17	29.3	236	$C_{16}H_{28}O$
18	30.4	268	$C_{18}H_{36}O$
19	31.7	282	$C_{19}H_{38}O$
20	32.8	296	$C_{20}H_{40}O$
21	33.8	310	$C_{21}H_{42}O$
22	34.3	324	$C_{22}H_{44}O$
23	34.9	338	$C_{23}H_{46}O$
24	35.5	352	$C_{24}H_{48}O$
25	35.9	380	$C_{26}H_{52}O$
26	36.2	262	$C_{17}H_{26}O_2$
27	36.9	394	$C_{25}H_{48}O_2$
28	37.2	402	$C_{27}H_{46}O_2$
29	37.7	352	$C_{22}H_{40}O_3$
30	38.1	288	$C_{21}H_{36}$
31	38.8	352	$C_{24}H_{48}O$
32	39.7	282	$C_{17}H_{30}O_3$
33	40.0	338	$C_{22}H_{42}O_2$
34	41.3	282	$C_{19}H_{38}O$
35	43.0	282	$C_{19}H_{38}O$
36	45.0	212	$C_{14}H_{28}O$
37	47.7	208	$C_{14}H_{24}O$
38	50.7	208	$C_{14}H_{24}O$
39	54.3	208	$C_{14}H_{24}O$

4. Discussion

Results of catalyst analyses by elemental and ICP methods were interpreted as most probable mixtures since the insoluble solids were not readily purified, refer to Table 2. Analysis of Catalyst B indicated it to be 70% $2Fe(CN)_2{\cdot}1.7K_3Cu(CN)_4{\cdot}2KCl$ from a combination of two similar products. Oxidized Catalyst A was indicated to be 75% $Fe(CN)_2OH{\cdot}Fe(CN)_2{\cdot}K_2Cu(CN)_3$ with one less ligand than the unoxidized catalyst, refer to Table 3.

Oily *n*-decane was catalytically air oxidized in nine sequential additions. Termination of catalytic oxidation of *n*-decane (after nine additions) demonstrated a total of 12.78 g (90 mmol) of *n*-decane had been added and 1 mmol of catalyst had caused approximately 11 g (approximately 80 mmol) of *n*-decane (corrected for evaporative losses) to be air oxidized with no measurable degradation in reaction rate. At the end of the first 5 h of catalytic oxidation a portion of the liquid was removed for analysis. The concentration of residual (extracted) *n*-decane was 73 mg in 100 mL, refer to Table 4. The aqueous portion containing suspended catalyst was reduced to a dry solid at approximately 80 °C. Its residual weight accounted for <50 mg of organic material.

An FT–IR spectrum of the solid residue exhibited absorption bands at 1655 and 1622 cm^{-1} indicating metal formate motion. Bands located at 2088 and 2047 cm^{-1} were associated with linear adsorbed CO motion. This indicated that a final result of oxidative catalysis was formation of carbon monoxide.

At the end of the entire catalytic oxidation sequence, again some 70 mg of residual *n*-decane and 1.6 mg of total extractable organic product were isolated indicating the other products had been lost by means of oxidation and/or evaporation. Less than 1.7 g of *n*-decane was lost at 16 + 1 °C by evaporation, 0.07 g remained un-reacted and 0.0016 g of oxidized product was extracted implying that some 11 g of products had been converted to gaseous products. The gas analysis detected no carbon dioxide, however, a substantial amount of carbon monoxide was detected by specific chemical absorption tube analyses and GC–MS analysis did indicate C_4, C_6, C_8–C_{11} compounds were present.

The GC–MS analysis of oxidized *n*-decane products extracted from the water phase demonstrated formation of complex aldehydes and unsaturated alcohols in the range of C_7–C_{26} of the general formulae $C_nH_{2n-2a}O$ ($n = 7$–19, $a = 0.1$), $C_nH_{2n-2a}O_2$ ($n = 7$–26, $a = 0.2$), $C_nH_{2n-2a}O_3$ ($n = 9$, $a = 0$) and C_nH_{2n-2a} for $n = 11$ and $a = 3$, refer to Tables 5 and 6.

n-Decane oxidized in a sealed 25 L Tedlar bag enclosure contained volatile organic products formed in the first 90 min of air oxidation. Measurements were

conducted for products in the solid, liquid and vapor phases, as well as that portion adsorbed on the walls of the enclosure for determination of a mass balance or accounting of these products. A 1.428 g weight (10 mmol) of the reactant, *n*-decane, was treated as 100 mmol of reactive carbon of which 8.12 mmol was available (i.e. not evaporated) for catalytic oxidation. Product analyses accounted for 7.10 mmol of the available 8.12 mmol reactant resulting in identification of 87% of the reacted carbon mass, refer to Tables 9 and 10. The reminder was believed associated with analysis of volatile products adsorbed on the walls of the enclosure and was probably lost during solvent evaporation. An evaporation test demonstrated that 91.88 mmol of un-reacted carbon became vaporized and was not available for catalytic oxidation.

Data found in Table 10 was rationalized as follows. The average weight of *n*-decane available from the first two columns of the first row was multiplied by the reaction rate to generate the amount of product formed in the second column. This algorithm was continued across the table to generate the weights of products formed. Thus, 1.272 g of *n*-decane was evaporated and 0.116 g (8.12 mmol of C) of oxidized organic products were formed. Carbon monoxide, acrolein, butanedial and other products detected by mass spectral and detector tubes accounted for 0.08 mmol (0.08 mmol of C). The FT–IR analysis of the 2 mmol of catalyst residue showed it to contain adsorbed carbon monoxide and iron formate accounting for 4 mmol of carbon monoxide (4 mmol of C). The interior walls of the Tedlar bag were extracted with reagent grade ethanol after the reaction was completed to isolate another 0.0432 g of products (3.02 mmol of C). This accounted for a total of 7.1 mmol of C product formation.

Catalytic air oxidation of hydrocarbons at ambient temperature demonstrated that aldehydes, carbon monoxide and water were formed in the absence of strong oxidizing agents [30]. The GC–MS analyses indicated these compounds might have been intermediate oxidation products since the total organic concentration resulting from extraction of products from 5 h oxidation of 1.42 g of *n*-decane was not >13.3 mg and decreased with reaction time to 1.6 mg indicating oxidation and loss of low molecular weight products of oxidation due to volatilization, refer to Fig. 1. A total of 12.8 g of *n*-decane was oxidized using 1 mmol of catalyst. Since some 10% of the *n*-decane was lost due to evaporation, then it may be concluded that approximately 11 g or 80 mmol of *n*-decane was catalytically oxidized and the final products were volatile aldehydes, carbon monoxide and water.

Peroxide oxidation of cyclohexane was reported to produce one $^{\bullet}$OH per each H_2O_2 consumed [17] indicating either $^{\bullet}$OH, MO^{1+} or MOH^{2+} to be the active species. Dimers formed during iron–hydroperoxide treatment of hydrocarbons [17] were reportedly consistent with oxidation by the hydroxyl radical. A hydroperoxo radical ($^{\bullet}O_2H$) intermediate [13,14,18] has been discussed in a chemical oxidation mechanism for conversion of liquid alkanes, by way of alkyl hydroperoxides, to aldehydes and alcohols. Other investigations focused on the function of transition metal complexes [31–34] as possible sources of a transient radical oxidizer of the form M–O_2H or M–OH. Methane has been reported to be oxidized [35] by O_2 and H_2O_2 to produce formaldehyde and other products presumably by $^{\bullet}$OH as well, while oxidation by the chlorite ion has been reported to oxidize formaldehyde to carbon dioxide and water [36]. Neither formaldehyde nor carbon dioxide was detected in this investigation indicating that these oxidations were not free radical reactions but were catalytic.

A series of catalytic oxidative reactions has been proposed to describe how the products in Table 6 may have been formed, refer to Table 9. A [cat] symbol represents the oxidative catalyst $[Fe(CN)_2L]\cdot[FeOH(CN)_2]$ as a source of reactive –OH groups. Water was omitted in Table 9 but CO was shown where needed. The oxidized version of the catalyst may be formed as shown.

$$2[Fe(CN)_2 \cdot L]_2 + \tfrac{1}{2}O_2 + H_2O \rightarrow 2[Fe(CN)_2(OH)\text{–}Fe(CN)_2 \cdot L] + 2L$$

This catalyst, and possibly its precursor, directed a series of related reactions to occur. Products identified in Tables 5–8 resulted from catalytic oxidation in formation of aldehydes, alcohols, alkenes, decarbonylation products, carbonylation products, bond cleavage and condensations. Each of these catalyzed reaction mechanisms will be treated herein.

Table 9
Rationalization of products formed as listed in Table 6

Line no.	Reactant	Column-entry	Oxidation reaction	Product	Column-entry
1	$C_{10}H_{22}$	Decane	$C_{10}H_{22} + 4[cat] \rightarrow C_9H_{19}CHO$	$C_{10}H_{20}O$	1–3, 5, 6 2–4
2	$C_{10}H_{20}O$	1–3, 5, 6, 2–4	$C_{10}H_{20}O + 4[cat] \rightarrow C_7H_{15}CH{=}CH{-}CHO$	$C_{10}H_{18}O$	1–4, 7
3	$C_{10}H_{18}O$	1–4, 7	$C_{10}H_{18}O + 2[cat] \rightarrow C_7H_{15}CHOH{-}CHOH{-}CHO \rightarrow C_7H_{15}CH_2{-}CO{-}CHO \rightarrow C_7H_{15}CH_2CHO + CO$	$C_9H_{18}O$	1–2
4	$C_9H_{18}O$	1–2	$C_5H_{11}CH_2CH_2CH_2CHO + 4[cat] \rightarrow C_5H_{11}CHOHCHOHCH_2CHO$	$C_9H_{18}O_3$	1–12, 2–7
5	$C_9H_{18}O_3 + C_9H_{18}O$	1–12, 2–7	$C_5H_{11}CHOHCHOHCH_2CHO + C_7H_{15}CH_2CHO \rightarrow C_5H_{11}C(CHO)(CH_2CH_2CHO)CH_2CH{=}CHC_5H_{11}$	$C_{18}H_{32}O_2$	(Table 4–5)
6	$C_{10}H_{20}O$	1–3, 5, 6, 2–4	$C_5H_{11}CH_2CH_2CH_2CH_2CHO + 6[cat] \rightarrow C_5H_{11}CH{=}CHCH_2CH_2CHO \rightarrow C_5H_{11}CHO + CHOCH_2CH_2CHO$	$C_6H_{12}O{+}C_4H_6O_2$	2–2, 3
7	$C_{10}H_{22}$	Decane	$C_{10}H_{22} + CO + [cat] \rightarrow C_{10}H_{21}CHO$	$C_{11}H_{22}O$	1–8
8	$C_{11}H_{22}O$	1–8	$C_7H_{15}CH_2CH_2CH_2CHO + 2[cat] \rightarrow C_7H_{15}CH_2CHOHCH_2CHO$	$C_{11}H_{22}O_2$	1–11
9	$C_{10}H_{22}$	Decane	$C_{10}H_{22} + 8[cat] \rightarrow CH_3CH_2CHOHCH_2CHOHCH_2CHOHCH_2CHOHCH_3$	$C_{10}H_{22}O_4$	–
10	$C_{10}H_{22}O_4$	–	$CH_3CH_2CHOHCH_2CHOHCH_2CHOHCH_2CHOHCH_3 + [cat] \rightarrow CH_3CH{=}CHCH{=}CHCH{=}CHCH{=}CHCH_3$	$C_{10}H_{14}$	2–5
11	$C_{10}H_{14}$	2–5	$CH_3CH{=}CHCH{=}CHCH{=}CHCH{=}CHCH_3 + [cat] \rightarrow CH_3CH{=}CHCH{=}CHCH{=}CHCH{=}CHCHO$	$C_{10}H_{12}O$	–
12	$C_{10}H_{12}O$	–	$CH_3CH{=}CHCH{=}CHCH{=}CHCH{=}CHCHO + [cat] \rightarrow CH_3CH{=}CHCH{=}CHCH{=}CHCH{=}CH_2 + CO$	C_9H_{12}	2–4
13	$C_{10}H_{22}$	Decane	$C_{10}H_{22} + 2[cat] \rightarrow C_5H_{11}CHOHCH_2C_3H_7$	$C_{10}H_{22}O$	–
14	$C_{10}H_{22}O$	–	$C_5H_{11}CHOHCH_2C_3H_7 + [cat] \rightarrow C_5H_{11}CH{=}CHC_3H_7$	$C_{10}H_{20}$	–
15	$C_{10}H_{20}$	–	$C_5H_{11}CH{=}CHC_3H_7 + 4[cat] \rightarrow C_5H_{11}CHO + CHOC_3H_7$	$C_6H_{12}O + C_4H_8O$	2–3
16	C_4H_8O	–	$CH_3CH_2CH_2CHO + 4[cat] \rightarrow CHOCH_2CH_2CHO$	$C_4H_6O_2$	2–2
17	$C_4H_6O_2$	2–2	$CHOCH_2CH_2CHO + 4[cat] \rightarrow CH_2{=}CHCHO$	C_3H_4O	2–1
18	$C_{11}H_{22}O$	1–8	$C_5H_{11}CH_2CH_2CH_2 + [cat] \rightarrow$ 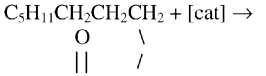 $C_5H_{11}CH{=}CHCH_2CH_2CH{=}CH_2$	$C_{11}H_{16}$	1–9, 10

Table 10
Mass balance of *n*-decane and products in Tedlar bag at 30 ± 2 °C (values in grams unless otherwise noted)

Component	0 min	30 min	60 min	90 min	Carbon equivalent (mmol)
Available *n*-decane reactant	1.428	0.965	0.503	0.040	100 Initially
Reaction rate[a]	0.053	0.053	0.053	0.053	–
Products formed (see text)	–	0.063	0.039	0.014	–
Total products (sum of row 3)	–	–	–	0.116	8.12
CO on 2 mmol of catalyst	–	–	–	4.00 mmol	4.00
Acrolein in vapor	–	–	–	27 ppm[b]	0.03
Butanedial in vapor	–	–	–	26 ppm[b]	0.03
Other compounds in vapor	–	–	–	20 ppm[b]	0.02
Residue on chamber walls	–	–	–	0.0432	3.02
Total C based account	–	–	–	–	(7.10/8.12) = 87%

[a] Refer to Fig. 1.
[b] ppm is parts per million or μg/gm.

Aldehydes can be formed by oxidative attack on primary hydrogen atoms as:

$$C_9H_{19}CH_3 + 4[Fe(CN)_2(OH)\text{–}Fe(CN)_2 \cdot L] + 4L \rightarrow C_9H_{19}CH(OH)_2 + 2H_2O + 4[Fe(CN)_2 \cdot L]_2 \rightarrow C_9H_{19}CHO + H_2O$$

See example on row 1 of Table 9.

Aldehydes may also be formed by carbonylation [37] indicated as:

$$C_9H_{19}CH_3 + Fe(CN)_2(COOH)\text{–}Fe(CN)_2 \cdot L \rightarrow C_9H_{19}CH_2CHO + Fe(CN)_2(OH)\text{–}Fe(CN)_2 \cdot L$$

See row 7 in Table 9. Both carbonylation and decarbonylation reactions have been observed on the same catalyst [38,39]. Carbonylation is commonly observed under reducing conditions as hydroformylation in the Fischer–Tropsch reaction [27].

Alcohols may be formed by oxidative attack on a secondary hydrogen atom as:

$$C_8H_{17}CH_2CH_3 + 2[Fe(CN)_2(OH)\text{–}Fe(CN)_2 \cdot L] \rightarrow C_8H_{17}CHOHCH_3 + 2[Fe(CN)_2\text{–}Fe(CN)_2 \cdot L] + H_2O$$

See rows 4 and 8 in Table 9.

Alkenes can result from elimination of water from an alcohol as:

$$C_7H_{15}CH_2CHOHCH_3 \xrightarrow{[cat]} C_7H_{15}CH = CHCH_3 + H_2O$$

See rows 5, 10 and 14 in Table 9. Alkenes have also been reported to be a by-product of decarbonylation [37–39].

Decarbonylation has been reported [37,38] by heating aldehydes in the presence of Wilkinson's catalyst ejecting carbon monoxide while leaving a hydrocarbon as:

$$C_9H_{19}CHO \xrightarrow{[cat]} C_9H_{20} + CO$$

See rows 3 and 12 in Table 9. Decarbonylation with Wilkinson's catalyst has been shown to proceed by a non-radical process [40] and catalytic products of formation have been verified [41,42]. Decarbonylation has also been reported by heating with organic peroxides.

Liquid olefins are subject to cleavage forming short chain aldehydes [43] in the presence of ozone rich oxygen and water. In this work, unsaturated compounds were cleaved by catalytic oxidative attack as:

$$C_5H_{11}CH = CHCH_2CH_2CH_3 + 4[Fe(CN)_2(OH)\text{–}Fe(CN)_2 \cdot L] + 4L \rightarrow C_5H_{11}CHO + OCHCH_2CH_2CH_3 + 2H_2O + 4[Fe(CN)_2 \cdot L\text{–}Fe(CN)_2 \cdot L]$$

See rows 6 and 15 in Table 9.

The FT–IR absorptions near 1556 cm^{-1} indicated formation of a chelated aldehyde and absorption near 1515 cm^{-1} has been attributed to the C=C bond [28]. Formation of secondary alcohols was observed by FT–IR as unsaturated alcohols as interpreted from the mass spectra.

Catalyst bonding to an alcohol or the enol form of an aldehyde created by means of a keto-enol tautormerism required the presence of an alpha hydrogen atom so subsequent catalyzed oxidation reaction sequences could produce a distribution of higher molecular weight aldehydes by an Aldol addition process [43,44] as indicated

$$C_5H_{11}CHO \rightleftharpoons C_4H_9CH = CHOH$$

$$C_4H_9CH_2CHO + CHOH = CHC_4H_9$$

$$\rightarrow C_4H_9CH(CHO)–CH(OH)CH_2C_4H_9$$

See row 5, Table 9. Addition reactions are indicated between an aldehyde and an unsaturated hydrocarbon as well [44] for the formation of other higher molecular weight products.

Atmospheric hexanes reacted in a similar manner except that a majority of the initial hexanes were lost by evaporation. Results of GC concentration measurements showed the isolated hexane concentrations to be indistinguishable from results of rapid vaporization of hexane from a blank run. Analysis of oxidized hexane products, extracted from the water phase, conducted by GC–MS procedures, demonstrated the formation of complex aldehydes and unsaturated alcohols in the range of C_6–C_{26} of the general formulae $C_nH_{2n-2a}O$ (n = 6–21, a = 0.1), $C_nH_{2n-2a}O_2$ (n = 16–26, a = 0.1) and $C_nH_{2n-2a}O_3$ (n = 12–26, a = −1.0, 1.2 or 6) quite similar to oxidized hydrocarbon products identified in *n*-decane catalytic oxidation residues, refer to Table 7.

A GC–MS chromatogram of the extract of hexanes oxidized at 7 atmospheres pressure, refer to Fig. 3, produced a complex, bimodal distribution of more than 40 narrow, regularly spaced peaks on top of two broad modal shapes, refer to products identified in Table 8. Interpretation of the MS data generated for each major narrow peak indicated the products to be in the C_6–C_{27} range. The products are represented by the general formulae $C_nH_{2n-2a}O$ for n = 14–26 and a = 1–3, $C_nH_{2n-2a}O_2$ for n = 9–27 and a = 0–4, $C_nH_{2n-2a}O_3$ for n = 6–22 and a = −1–2, and C_nH_{2n-2a} for n = 14 and 21, and a = 2–3. The GC–MS inlet temperature was reduced to just vaporize the products to avoid possible product degradation with similar results. A 10 ml portion of the oxidized hexanes extract was reduced to alcohols with 0.2 g of sodium borohydride in 50 ml of deionized water with 15 min of stirring. The resulting product was extracted with 10 ml of reagent grade dichloromethane for analysis and GC–MS measurements proved the products to be >99% alcohols in the C_6–C_{24} range, thus, verifying the original GC–MS results for aldehydes.

Catalyst free ultrasonic treatment of hydrocarbons was ineffective using tap water that contained <0.01 ppm of Fe and Cu, even after 30 min of ultrasonic agitation, where as tap water containing Cu and Fe in the 0.5–2.0 ppm range did affect hydrocarbon oxidation. From these results, it was clear that ultrasonic energy alone did not degrade hydrocarbons without the aid of a catalyst. These were catalytic oxidations, not ultrasonic degradations.

Catalytic air oxidation of aliphatic hydrocarbons at ambient conditions can form aldehydes, secondary alcohols and other products, and can completely destroy the hydrocarbon forming carbon monoxide and water. Non-hazardous catalysts, of the form described herein, were used to destroy 100 mg/kg gasoline, diesel fuel, jet fuel and kerosene in soil. Subsequent GC analysis of concentrated soil extracts demonstrated hydrocarbon concentrations to be reduced to <1 mg/kg in a 17 day period at 10–16 °C.

5. Conclusions

Catalytic ambient air oxidation of aliphatic hydrocarbons has been demonstrated where a majority of products formed were carbon monoxide, water and volatile oxidized products. Novel catalysts, such as $[Fe(CN)_2(OH)]\cdot[Fe(Cl)_2L]$, have been produced in the laboratory and demonstrated to effectively air oxidize hexanes, *n*-decane, gasoline and diesel fuel. This is believed to be the first such demonstration of catalytic air oxidation of hydrocarbons at ambient temperature and pressure. It is hoped that this work will add to the existing body of catalysis knowledge, give the chemical industry new opportunities for development of more efficient catalysts and provide a growth opportunity for industrial catalytic air oxidation of hydrocarbons.

References

[1] K. Blau, O. Kovacs, G. Lauterbach, M. Makhoul, W. Pritzkow, T.D. Tien, J. Prakt. Chem. 351 (1989) 771.

[2] F. Garcia-Ochoa, A. Romero, J. Querol, Chem. Eng. J. 43 (1990) 33.
[3] B. Kraushaar-Czarnetzki, W.G.M. Hoogervorst, W.H.J. Stork, Stud. Surf. Sci. Catal. 84 (1994) 1869.
[4] T.-C. Lau, C.-K. Mak, J. Chem. Soc., Chem. Commun. 766 (1993);
T.-C. Lau, C.-K. Mak, J. Chem. Soc., Chem. Commun. 943 (1995).
[5] S. Giddings, A. Mills, J. Org. Chem. 53 (1988) 1103.
[6] T. Tatsumi, M. Nakamura, S. Negishi, H.-O. Tominaga, J. Chem. Soc., Chem. Commun. 476–477 (1990).
[7] J.S. Reddy, S. Sivasanker, Catal. Lett. 11 (1991) 241–244.
[8] P.R.H.P. Rao, A.V. Ramaswamy, J. Chem. Soc., Chem. Commun. 1245–1246 (1992).
[9] D.R.C. Huybrechts, L. De Bruycker, P.A. Jacobs, Nature 345 (1990) 240–242.
[10] M.G. Clerici, Appl. Catal. 68 (1991) 249–261.
[11] A. Corma, M.A. Camblor, P. Esteve, A. Martinez, J. Perez-Pariente, J. Catal. 145 (1994) 151–158.
[12] P.R.H.P. Rao, A.V. Ramaswamy, P. Ratnasamy, J. Catal. 141 (1993) 604–611.
[13] M. Bressan, L. Forti, A. Morvillo, Inorg. Chim. Acta 211 (1993) 217.
[14] G.B. Shulpin, M.M. Bochkova, G.V. Nizova, J. Chem. Soc., Perkin Trans. 2 (1995) 1465.
[15] C. Walling, Acc. Chem. Res. 8 (1975) 125.
[16] C. Walling, et al., Inorg. Chem. 9 (1970) 931;
C. Walling, et al., J. Am. Chem. Soc. 93 (1971) 4275.
[17] D.L. Ingles, Aust. J. Chem. 26 (1973) 1015;
D.L. Ingles, Aust. J. Chem. 26 (1973) 1021.
[18] C. Sheu, A. Sobkowiak, L. Zhang, N. Ozbalik, D.H.R. Barton, D.T. Sawyer, J. Am. Chem. Soc. 111 (1989) 8030–8032.
[19] C. Sheu, A. Sobkowiak, S. Jeon, D.T. Sawyer, J. Am. Chem. Soc. 112 (1990) 879–881.
[20] J.B. Vincent, J.C. Huffman, G. Christou, Q. Li, M.A. Nanny, D.N. Hendrickson, R.H. Fong, R.H. Fish, J. Am. Chem. Soc. 110 (1988) 6898–6900.
[21] C. Sheu, D.T. Sawyer, J. Am. Chem. Soc. 112 (1990) 8212–8214.
[22] N. Kitajima, H. Fukui, Y. Moro-oka, J. Chem. Soc., Chem. Commun. 485–6 (1988).
[23] M.P. Woodland, D.S. Patel, R. Cammack, H. Dalton, Biochim. Biophys. Acta 873 (1986) 237.
[24] A.C. Rosenzweig, C.A. Frederick, S.J. Lippard, P. Nordlund, Crystal structure of a bacterial non-haem iron hydroxylase that catalyses the biological oxidation of methane, Nature 366 (1993) 537–543.
[25] M.K. Carter, An investigation of the concepts of catalysis, in preparation.
[26] F.A. Cotton, G. Wilkinson, Advanced Inorganic Chemistry, 4th ed., Wiley, New York, 1980, pp. 63, 1050.
[27] M.K. Carter, J. Mol. Catal. Part A: Chem. 172 (2001) 193–206.
[28] L.J. Bellamy, The Infrared Spectra of Complex Molecules, Chapman and Hall, New York, 1975, p. 165.
[29] R.C. Weast, CRC Handbook of Chemistry and Physics, 65th ed., CRC Press Inc., Boca Raton, FL, 1985, Sect. F, p. 202.
[30] M.K. Carter, US Patent Application filed 2001.
[31] I.M. Kolthoff, A.I. Medalia, J. Am. Chem. Soc. 71 (1949) 3777, 3784, 3789.
[32] G. Balavoine, D.H.R. Barton, J. Boivin, A. Gref, N. Ozbalik, H. Riviere, Tetrahedron Lett. 27 (25) (1986) 2849–2852.
[33] C. Sheu, S.A. Richert, P. Cofre, B. Ross Jr., A. Sobkowiak, D.T. Sawyer, J.R. Kanofsky, J. Am. Chem. Soc. 112 (1990) 1936–1942.
[34] D.H.R. Barton, E. Csuhai, D. Dollar, Y. Geletii, Tetrahedron 47 (33) (1991) 6561–6570.
[35] G. Suss-Fink, G.V. Nizova, S. Stanislas, G.B. Shulpin, J. Mol. Catal. Part A: Chem. 130 (1998) 163.
[36] C.R. Chinake, O. Olojo, H. Simoyi, J. Phys. Chem. A 102 (1998) 606.
[37] K. Ohno, J. Tsuji, J. Am. Chem. Soc. 90 (1949) 99.
[38] M.C. Baird, C.J. Nyman, G. Wilkinson, J. Chem. Soc. A 348 (1968).
[39] J. Tsuji, K. Ohno, Tetrahedron Lett. 3969 (1965).
[40] J.A. Kampmeier, S.H. Harris, I. Wedegaertner, J. Org. Chem. 45 (1980) 315.
[41] J.W. Suggs, J. Am. Chem. Soc. 100 (1978) 640.
[42] J.A. Kampmeier, S.H. Harris, I. Mergelsberg, J. Org. Chem. 49 (1984) 621.
[43] C.R. Noller, Chemistry of Organic Compounds, W.B. Saunders Company, Philadelphia, 1957, p. 205.
[44] E.S. Gould, Mechanism and Structure in Organic Chemistry, Henry Holt and Company, New York, 1959, p. 389.